Filomat 39:15 (2025), 5285–5296
https://doi.org/10.2298/FIL2515285V

Published by Faculty of Sciences and Mathematics,
University of Niš, Serbia
Available at: http://www.pmf.ni.ac.rs/filomat

An analytical approach to determining crossing and veering phenomena

Marko A. Veg[a,*], Aleksandar M. Tomović[a], Danilo Z. Karličić[b]

[a]*Faculty of Mechanical Engineering, University of Belgrade, 11000 Belgrade, Serbia*
[b]*Mathematical Institute of the Serbian Academy of Sciences and Arts, 11000 Belgrade, Serbia*

Abstract. The aim of this paper is to give formal analytical proof of the crossing phenomena in the case of a planar frame structure that consists of two Euler-Bernoulli beams. The criteria for distinguishing veering from crossing are presented. It is supposed that frame elements are made of homogeneous materials and with circular cross section. An analytical approach to solving the problem is applied with respect to the Euler-Bernoulli beam theory, thus no discretization techniques were used. The variable system parameter is the diameter of the cross sections. For different values of the diameter eigenvalue loci may cross or abruptly diverge – veer apart. Based on the matrix transformation known from linear algebra the analytical solution for the presented problem is proposed and illustrated by an example.

1. Introduction

Computation of natural frequencies is an omnipresent procedure in structural dynamics where discretization-based numerical procedures are mostly used. The implementation of such procedures in calculation of natural frequencies of structural elements can lead to some misconceptions. The change of a system parameter is followed by changes in natural frequencies. When a system parameter changes a family of eigenvalue loci can be plotted, where two lines can approach each other and cross or abruptly diverge – veer apart. When two natural frequencies approach each other, they often veer apart, instead of crossing [1]. The purpose of this paper was partly to describe the general circumstances concerning whether or not veering occurs, as in [2]. Due to discretization and numerical imperfections, one may observe veering as crossing or vice versa. Although a physical phenomenom, apparent veering can be a consequence of model discretization. The free vibration analysis of planar frame structures composed of Euler-Bernoulli beams interconnected with rigid bodies was considered in [3] where orthogonality conditions of mode shapes were derived as well. The general case of mass center displacement with respect to beam neutral axes was

2020 *Mathematics Subject Classification*. Primary: 74K10.
Keywords. eigenvalue loci, crossing, veering, Euler-Bernoulli beam theory, matrix rank
Received: 27 December 2023; Revised: 16 September 2024; Accepted: 12 March 2025
Communicated by Marko Petković
Support for this research was provided by the Ministry of Education, Science and Technological Development of the Republic of Serbia under Grants Nos. 451-03-47/2023-01/200105 and 451-03-47/2023-01/200108. This support is gratefully acknowledged.
* Corresponding author: Marko A. Veg
Email addresses: mveg@mas.bg.ac.rs (Marko A. Veg), atomovic@mas.bg.ac.rs (Aleksandar M. Tomović), danilok@turing.mi.sanu.ac.rs (Danilo Z. Karličić)
ORCID iDs: https://orcid.org/0000-0002-5308-6122 (Marko A. Veg), https://orcid.org/0000-0002-8462-8086 (Aleksandar M. Tomović), https://orcid.org/0000-0002-7547-9293 (Danilo Z. Karličić)

considered thus leading to coupling in axial and transverse mode shapes. Planar frame structures composed of Euler-Bernoulli beams with variable mechanical and geometric parameters were studied in [4]. Coupling of axial and transverse vibration is discussed due to boundary conditions and a procedure is proposed for reducing the mathematical problem to a system of ordinary differential equations and solving it. The effect of axial and transverse vibration is considered for Timoshenko beams in [5], along with the presented model the eigenvalue veering phenomenon is investigated. A continuum model given for the structure of two cantilever beams is presented in [6]. Eigenfrequencies were computed directly and a comprehensive study of eigenfrequency loci veering and mode splitting is conducted. The influence of various parameters to loci veering and crossing was studied. Authors have shown in [7] that small structural disorder of nearly periodic structures results in strong localization of mode shapes and mutual repulsion of eigenvalues loci. It was presented in [8] that design often involves placing constraints on the natural frequencies of the system or on its components. In [9] the curve veering of cable-stayed and suspension bridge frequency loci is studied. The perturbation series solution is used to examine the variations in eigenvalues due to minor changes of system parameters. It is shown that the concept of curve veering in bridge natural frequency loci enables better insights in the underlying physics of their aeroelastic behavior. In [10] authors gave a theoretical and experimental analysis of a non-symmetric structure with eigenvalues curve veering and crossing. Based on the known literature examples, the numerical finite element (FE) model was developed to describe a tunable and simple test rig. The test rig is made of simple beams and masses, with a tunable angle of the intermediate beam. In [11] authors compared results obtained in an experimental setup with those from FE analysis using a symmetric and an asymmetric model. The satisfying results matching are observed using asymmetric model where loci veering is detected as in the experimental analysis. Symmetric model leads toward loci crossing which may be the error due to numerical model approximation. Authors proposed three analytical criteria for numerical classification of veering, namely: cross-sensitivity quotient, modal dependence factor and the veering index in [2]. The advantages of isogeometric analysis to Finite Element Analysis in studying crossing and veering phenomena are discussed in [12]. The computational results are compared to the experimental ones for different configuration and dynamic coupling. The procedure for prediction of modal parameters in case of mode crossing and veering with variation of structural parameters is proposed in [13]. In [14] authors discuss curve veering and crossing phenomena with respect to both approximate and analytical solutions. They propose approximate values of the physical system to be treated as the exact values of a fictitious system and when approximation is minimized, previously seen veering behavior in some cases vanishes. Results of the practical experiment for mode veering, crossing and lock-in phenomena were presented in [15]. The evidence of damping-dependent transition from veering to crossing is investigated for a system that consists of two beams. The crossing and veering phenomena for the specific mechanical structure are discussed in [16] where both numerical simulations and experimental tests were used to evaluate the phenomena. Eigenfrequency veering of a system of two overhanged beams was studied in [17]. An analytical method for eigenfrequency computation was derived thus avoiding discretization. It can be noted that the error that goes with discretization procedures can lead to wrong results because of two eigenfrequencies that are close one to one another. The effects of overhang to mode coupling were also discussed. In [18] authors study two disordered nearly periodic structures and show that small structural irregularities result in strong localization of mode shapes and mutual repulsion of the loci of eigenvalues, so abrupt veering is noticed when eigenvalues are plotted with respect to the parameter of structural disorder. The second derivative of an eigenvalue function and the first derivative of an eigenvector were taken as the measures in describing the phenomena of eigenvalue curve veering and mode localization in [19]. The phenomena occurs if eigenvalues are considered close. The example is presented for weakly coupled springs. The vibration analysis of an axially loaded cantilever beam by a tendon is conducted by the authors in [20]. Modelling was conducted using Euler-Bernoulli beam theory. The number of attachment points is shown to be crucial in frequency loci veering of beam-dominated vs tendon-dominated vibration modes. The system of two simple oscillators coupled by a spring was considered in [21], where Stephen introduced the concept of the center of veering and a procedure for transformation of coordinates. The procedure was presented to detect veering using coordinate transformations and geometric features of a hyperbola rather than using derivatives of eigenvalues and eigenvectors. The detailed discussion on the influence of various parameters on the emergence mode veering phenomenon for in-plane vibration of pre-stressed hexagonal

lattice embedded in an elastic medium with the application of Timoshenko beam theory was conducted in [22]. In this paper eigenvalue loci veering and crossing are studied for a planar frame structure that consists of two Euler-Bernoulli beams made of homogeneous materials and circular cross-sectional areas. The varied parameter is the beam diameter, which is equal for both beams. A specific example is considered and it can be shown that the procedure can be extended to a system of beams with intermittent bodies inserted between them, all in the boundaries of linear theory of elasticity, where the characteristic equation can be determined in analytic form. This procedure can also be applied to a spatial model of vibration.

2. Governing equations and boundary conditions

The planar frame structure in Fig. 1 consists of two Euler-Bernoulli beams AC and CB of equal length L, constant and equal circular cross sections of diameter D, equal elasticity modulus E and mass-density ρ. The beams are joined together in point C at an internal angle of 135°. Two stationary right-hand Cartesian coordinate systems $Ax_1y_1z_1$ and $Cx_2y_2z_2$ are placed at one end of each beam in the undeformed state, with the axes z_1 and z_2 aligned with the beams' axes. The longinutdinal displacements of cross-sections of beams 1 (AC) and 2 (CB) are given as $w_1(z_1, t)$ and $w_2(z_2, t)$, while the transverse displacements are given as $v_1(z_1, t)$ and $v_2(z_2, t)$ respectively (see Fig. 1).

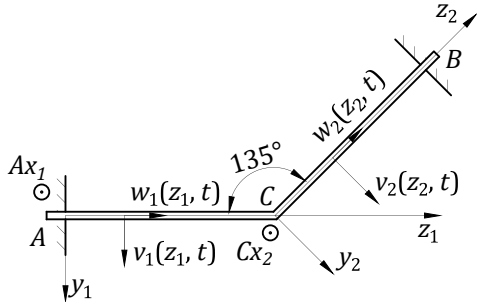

Figure 1: Planar frame.

The partial differential equations of longitudinal vibrations of beams AC and CB from [23] are given in eqs. (1), (2), while the longitudinal wave propagation velocities c_l, according to the material properities, are given in eq. (3):

$$\frac{\partial^2 w_1}{\partial t^2} - c_{l1}^2 \frac{\partial^2 w_1}{\partial z_1^2} = 0, \tag{1}$$

$$\frac{\partial^2 w_2}{\partial t^2} - c_{l2}^2 \frac{\partial^2 w_2}{\partial z_2^2} = 0, \tag{2}$$

$$c_l^2 = \frac{E}{\rho}, \omega_l = k_l c_l, k_l = p, E_1 = E_2 = E, \rho_1 = \rho_2 = \rho \Rightarrow c_{l1} = c_{l2} = c_l. \tag{3}$$

where ω_l is the angular frequency of longitudinal waves and k_l is the characteristic number. Equal longitudinal wave velocities due to the same material properties are presented in eq. (3) . The partial differential equations of transverse vibrations of beams AC and CB from [23] are given in equations (4), (5), and similarly

we get equal propagation velocities c_t of transverse waves from (6):

$$\frac{\partial^2 v_1}{\partial t^2} + c_{t1}^2 \frac{\partial^4 v_1}{\partial z_1^4} = 0, \tag{4}$$

$$\frac{\partial^2 v_2}{\partial t^2} + c_{t2}^2 \frac{\partial^4 v_2}{\partial z_2^4} = 0, \tag{5}$$

$$c_t^2 = \frac{EI_x}{\rho A}, \omega_t = k_t^2 c_t, k_t = k, A_1 = A_2 = \frac{D^2\pi}{4}, I_{x1} = I_{x2} = \frac{D^4\pi}{64}, \rho_1 = \rho_2 = \rho \Rightarrow c_{t1} = c_{t2} = c_t. \tag{6}$$

where ω_t is the angular frequency of transverse waves, k_t is the characteristic number, D is the beam diameter and A is the area of the cross-section. Based on the Euler-Bernoulli beam theory [23], cross sectional bending moments, axial and transverse forces are given in eqs. (7) - (9) respectively:

$$M_{f1}(z_1, t) = -EI_x \frac{\partial^2 v_1}{\partial z_1^2}, \quad M_{f2}(z_2, t) = -EI_x \frac{\partial^2 v_2}{\partial z_2^2}, \tag{7}$$

$$F_{A1}(z_1, t) = EA \frac{\partial w_1}{\partial z_1}, \quad F_{A2}(z_2, t) = EA \frac{\partial w_2}{\partial z_2}, \tag{8}$$

$$F_{T1}(z_1, t) = -EI_x \frac{\partial^3 v_1}{\partial z_1^3}, \quad F_{T2}(z_2, t) = -EI_x \frac{\partial^3 v_2}{\partial z_2^3}. \tag{9}$$

Boundary conditions are set by the clamp constraints at points A and B of the beam, and by the rigid joint in point C. Presented in Fig. 2 is a beam segment of infinitesimaly small length in point C, where α is the supplementary angle to the internal angle between the two beams, and is equal to 45°. Following in eqs. (10) are the boundary conditions of the clamped end in point A, where $z_1 = 0$ and where there are no axial and transverse displacements, and where there is no rotation angle for the entire time interval of vibration.

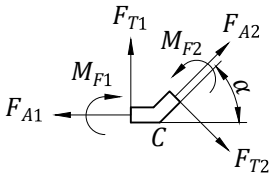

Figure 2: Cross sectional forces and moments.

For the clamped end in point A, the boundary conditions read:

$$w_1(0, t) = 0, \quad v_1(0, t) = 0, \quad v_1'(0, t) = 0. \tag{10}$$

From the equality of internal forces and moments in the cross section follow the boundary conditions in point C:

$$M_{f1}(l, t) = M_{f2}(0, t), \tag{11}$$

$$-F_{A1}(l, t) + F_{A2}(0, t)\cos\alpha + F_{T2}(0, t)\sin\alpha = 0, \tag{12}$$

$$F_{T1}(l, t) + F_{A2}(0, t)\sin\alpha - F_{T2}(0, t)\cos\alpha = 0. \tag{13}$$

Due to the rigid joint in point C, geometrical relations between displacements and rotational angles in the two coordinate systems are given in eqs. (14)-(16):

$$v_1'(l, t) = v_2'(0, t), \tag{14}$$

$$w_1(l, t) = w_2(0, t)\cos\alpha + v_2(0, t)\sin\alpha, \tag{15}$$

$$v_1(l, t) = v_2(0, t)\cos\alpha - w_2(0, t)\sin\alpha. \tag{16}$$

For the clamped end at point B, the boundary conditions read:

$$w_2(l,t) = 0, \quad v_2(l,t) = 0, \quad v_2'(l,t) = 0. \tag{17}$$

3. Differential equations' solutions and the characteristic equation

The general solutions of the governing differential equations, according to the method of separation of variables [23] read:

$$w_1 = Z_1(z_1)T_1^*(t), \quad v_1 = V_1(z_1)T_1(t), \tag{18}$$
$$w_2 = Z_2(z_2)T_2^*(t), \quad v_2 = V_2(z_2)T_2(t). \tag{19}$$

where $Z_1(z_1)$, $V_1(z_1)$, $Z_2(z_2)$ and $V_2(z_2)$ represent amplitudes of axial and bending displacements respecitevely, and $T_1^*(t)$, $T_1(t)$, $T_2^*(t)$, $T_2(t)$ time functions of longitudinal and transverse vibrations respectively. Now, after separation of variables, the cross-sectional forces and bending moments from (7) - (9) read:

$$M_{f1}(z_1,t) = -EI_x\frac{\mathrm{d}^2V_1(z_1)}{\mathrm{d}z_1^2}T_1(t), \quad M_{f2}(z_2,t) = -EI_x\frac{\mathrm{d}^2V_2(z_2)}{\mathrm{d}z_2^2}T_2(t), \tag{20}$$
$$F_{A1}(z_1,t) = EA\frac{\mathrm{d}Z_1(z_1)}{\mathrm{d}z_1}T_1^*(t), \quad F_{A2}(z_2,t) = EA\frac{\mathrm{d}Z_2(z_2)}{\mathrm{d}z_2}T_2^*(t), \tag{21}$$
$$F_{T1}(z_1,t) = -EI_x\frac{\mathrm{d}^3V_1(z_1)}{\mathrm{d}z_1^3}T_1(t), \quad F_{T2}(z_2,t) = -EI_x\frac{\mathrm{d}^3V_2(z_2)}{\mathrm{d}z_2^3}T_2(t). \tag{22}$$

Also, after separation of variables, the amplitude and time functions have the form shown in (23) - (30).

$$V_1(z_1) = C_1\cos(k_1z_1) + C_2\sin(k_1z_1) + C_3\cosh(k_1z_1) + C_4\sinh(k_1z_1), \tag{23}$$
$$Z_1(z_1) = C_5\cos(p_1z_1) + C_6\sin(p_1z_1), \tag{24}$$
$$V_2(z_2) = C_7\cos(k_2z_2) + C_8\sin(k_2z_2) + C_9\cosh(k_2z_2) + C_{10}\sinh(k_2z_2), \tag{25}$$
$$Z_2(z_2) = C_{11}\cos(p_2z_2) + C_{12}\sin(p_2z_2), \tag{26}$$

$$T_1^*(t) = A_1^*\cos(\omega_{l1}t) + B_1^*\sin(\omega_{l1}t), \tag{27}$$
$$T_1(t) = A_1\cos(\omega_{t1}t) + B_1\sin(\omega_{t1}t), \tag{28}$$
$$T_2^*(t) = A_2^*\cos(\omega_{l2}t) + B_2^*\sin(\omega_{l2}t), \tag{29}$$
$$T_2(t) = A_2\cos(\omega_{t2}t) + B_2\sin(\omega_{t2}t). \tag{30}$$

From the boundary conditions in (10), relations (31) - (33) are obtained as follows:

$$Z_1(0) = 0 \Rightarrow C_5 = 0, \tag{31}$$
$$V_1(0) = 0 \Rightarrow C_1 + C_3 = 0, \tag{32}$$
$$V_1'(0) = 0 \Rightarrow C_2 + C_4 = 0. \tag{33}$$

From the boundary conditions in (17) , relations (34) - (36) are obtained as follows:

$$Z_2(l) = 0 \Rightarrow C_{11}\cos(p_2l) + C_{12}\sin(p_2l) = 0, \tag{34}$$
$$V_2(l) = 0 \Rightarrow C_7\cos(k_2l) + C_8\sin(k_2l) + C_9\cosh(k_2l) + C_{10}\sinh(k_2l) = 0, \tag{35}$$
$$V_2'(l) = 0 \Rightarrow -k_2C_7\sin(k_2l) + k_2C_8\cos(k_2l) + k_2C_9\sinh(k_2l) + k_2C_{10}\cosh(k_2l) = 0. \tag{36}$$

From the boundary condition (11) follows the equality $T_1(t) = T_2(t)$ of time functions of transverse vibrations of the two beams, because the equality of flexural moments must hold for the entire time interval of motion. Similarly, from the boundary condition (13) follows the equality $T_2^*(t) = T_2(t)$ of time functions on beam

CB, and finally from the boundary condition (12) follows the equality of time functions $T_1^*(t) = T_2^*(t)$. As a consequence of these boundary conditions, longitudinal and transverse vibrations are coupled and the equality of natural frequencies follows as given in (37):

$$T_1^*(t) = T_1(t) = T_2(t) = T_2^*(t) = T(t) \Rightarrow \omega_t = \omega_l \Rightarrow p = k^2\sqrt{\frac{I_x}{A}} = \frac{1}{4}k^2 D. \tag{37}$$

Now, the solutions of governing differential equations are:

$$w_1 = Z_1(z_1)T_1^*(t) = Z_1(z_1)T(t), \tag{38}$$
$$v_1 = V_1(z_1)T_1(t) = V_1(z_1)T(t), \tag{39}$$
$$w_2 = Z_2(z_2)T_2^*(t) = Z_2(z_2)T(t), \tag{40}$$
$$v_2 = V_2(z_2)T_2(t) = V_2(z_2)T(t). \tag{41}$$

From boundary conditions (10), which have the general form $f_i = f_i(C_1, C_2, \ldots, C_6) = 0$, $i = 1, 2, 3$ it is possible to determine the integration constants C_3, C_4 and C_5 as:

$$C_3 = \Phi_1(C_1, C_2, C_6), \tag{42}$$
$$C_4 = \Phi_2(C_1, C_2, C_6), \tag{43}$$
$$C_5 = \Phi_3(C_1, C_2, C_6). \tag{44}$$

From boundary conditions (11) - (16), which have the general form $f_i = f_i(C_1, C_2, \ldots, C_{12}) = 0$, $i = 4, \ldots, 9$, it is possible to determine the integration constants C_7, C_8, $\ldots$, C_{12} as:

$$C_7 = \Psi_1(C_1, \ldots, C_6), \tag{45}$$
$$C_8 = \Psi_2(C_1, \ldots, C_6), \tag{46}$$
$$\vdots \tag{47}$$
$$C_{12} = \Psi_6(C_1, \ldots, C_6). \tag{48}$$

Boundary conditions at point B (17), which have the general form $f_i = f_i(C_7, C_8, \ldots, C_{12}) = 0$, $i = 10, \ldots, 12$. When substituting (45) - (48) into the (17), we get:

$$f_i = f_i(C_1, \ldots, C_6) = 0, \text{for } i = 10, 11, 12. \tag{49}$$

After substituting (42) - (44) into (49), a homogenous system of linear equations in terms of C_1, C_2 and C_6 is obtained:

$$\begin{aligned} K_{11}(k, D)C_1 + K_{12}(k, D)C_2 + K_{13}(k, D)C_6 &= 0, \\ K_{21}(k, D)C_1 + K_{22}(k, D)C_2 + K_{23}(k, D)C_6 &= 0, \\ K_{31}(k, D)C_1 + K_{32}(k, D)C_2 + K_{33}(k, D)C_6 &= 0. \end{aligned} \tag{50}$$

or presented in matrix form $\mathbf{K}(k, D)\mathbf{C} = \mathbf{0}$, where:

$$\mathbf{K}(k, D) = \begin{pmatrix} K_{11} & K_{12} & K_{13} \\ K_{21} & K_{22} & K_{23} \\ K_{31} & K_{32} & K_{33} \end{pmatrix}, \text{and } \mathbf{C} = \begin{pmatrix} C_1 \\ C_2 \\ C_6 \end{pmatrix}. \tag{51}$$

To further simplify the equations, the following abbreviations are introduced:

$$\cos kl = Co,\ \sin kl = Si,\ \cosh kl = Ch,\ \sinh kl = Sh, \tag{52}$$
$$\cos pl = \cos\left(\frac{Dk^2 l}{4}\right) = a,\ \sin pl = \sin\left(\frac{Dk^2 l}{4}\right) = b. \tag{53}$$

From (50), with using the abbreviations introduced in (52), the elements of the **K** matrix are:

$$K_{11} = -\frac{1}{4}\left(Ch^2(\sqrt{2}+2) - Co^2(\sqrt{2}+2) + Sh^2(\sqrt{2}+2) + Sh\,Si(4-2\sqrt{2}) + Si^2(\sqrt{2}+2)\right), \tag{54}$$

$$K_{12} = -\frac{1}{2}\left(Ch\,Sh(\sqrt{2}+2) - Ch\,Si(\sqrt{2}-2) + Co\,Sh(\sqrt{2}-2) - Co\,Si(\sqrt{2}+2)\right), \tag{55}$$

$$K_{13} = \frac{1}{4Dk}\left(4\sqrt{2}Si\,a - 4\sqrt{2}Sh\,a + \sqrt{2}Ch\,Dbk + \sqrt{2}Co\,Dbk\right), \tag{56}$$

$$K_{21} = -\frac{1}{2}k\left(Ch\,Sh(\sqrt{2}+2) - Ch\,Si(\sqrt{2}-2) - Co\,Sh(\sqrt{2}-2) + Co\,Si(\sqrt{2}+2)\right), \tag{57}$$

$$K_{22} = -\frac{1}{4}k\left(Ch^2(\sqrt{2}+2) - Co^2(\sqrt{2}+2) + Sh^2(\sqrt{2}+2) + Sh\,Si(4-2\sqrt{2}) + Si^2(\sqrt{2}+2)\right), \tag{58}$$

$$K_{23} = -\frac{1}{4D}\left(4\sqrt{2}Ch\,a - 4\sqrt{2}Co\,a - \sqrt{2}Sh\,Dbk + \sqrt{2}Si\,Dbk\right), \tag{59}$$

$$K_{31} = \frac{1}{8}\left(4\sqrt{2}Ch\,a - 4\sqrt{2}Co\,a - \sqrt{2}Sh\,Dbk + \sqrt{2}Si\,Dbk\right), \tag{60}$$

$$K_{32} = -\frac{1}{8}\left(4\sqrt{2}Si\,a - 4\sqrt{2}Sh\,a + \sqrt{2}Ch\,Dbk + \sqrt{2}Co\,Dbk\right), \tag{61}$$

$$K_{33} = \sqrt{2}ab. \tag{62}$$

An analysis of matrix **K** elements shows the following relations between its elements:

$$K_{32} = -\frac{kD}{2}K_{13}, \tag{63}$$

$$K_{31} = -\frac{D}{2}K_{23}, \tag{64}$$

$$K_{22} = kK_{11}. \tag{65}$$

For the homogenous system in eq. (50) to have non-trivial solutions, the determinant of the system has to be equal to zero. It is a transcendent equation in terms of the characteristic number k and, in the case considered in this paper, of the diameter of the beam cross-section D as the varied parameter. In the general case the equation has an infinite number of solutions k_n, for $n = 1, \ldots, \infty$. The determinant of the system is given in (66). This paper investigates if it is possible to find multiple roots for a specific value of the parameter D, that is to lose a mode of vibration.

$$|\mathbf{K}| = \begin{vmatrix} K_{11} & K_{12} & K_{13} \\ K_{21} & K_{22} & K_{23} \\ K_{31} & K_{32} & K_{33} \end{vmatrix} = 0. \tag{66}$$

The second order cofactors of matrix **K** are determined as:

$$\Delta_{ij} = (-1)^{i+j}M_{ij}, \tag{67}$$

where M_{ij} is the minor of **K** obtained by taking the determinant of **K** with row i and column j removed.

4. Analytic proof of crossing

The function $f(k, D) = |K|$ has an infinite number of zero crossings for k_n, where $n = 1, \ldots, \infty$. If graphed, by varying the parameter D, we're looking for some D^* that would bear two equal characteristic numbers $k_n = k_{n+1}$. This means efectively bringing together two adjacent characteristic numbers on the graph as to get one zero crossing instead of two, and having the function $f(k, D^*)$ touch the k-axis in the point $k_n = k^*$ (Fig. 3).

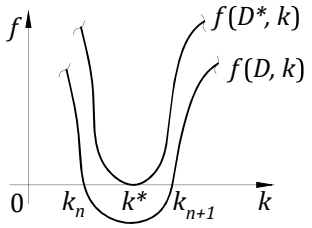

Figure 3: Graph representation of $f(D, k)$.

Numerically, this can be done by solving the system of equations (68).

$$\begin{aligned} f(k, D) &= 0 \text{ and} \\ \frac{\partial f(k, D)}{\partial k} &= 0, \end{aligned} \tag{68}$$

where it is possible to solve for k^* and D^*. Using the inbuilt function *FindRoot* in *WolframMathematica*, which accepts a system of equations along with proposed neighbourhoods for the values of k^* and D^*, it is possible to determine D^* and k^* for two arbitrary characteristic numbers k_n and k_{n+1}. It is natural to look for multiple zeros somewhere between the first few modes, which has to be kept in mind when using *FindRoot*. Also, it is possible to numerically show that the values D^* and k^*, determined using *FindRoot*, are the roots of an arbitrary system of equations (69).

$$\begin{aligned} &\Delta_{ij} = 0, \\ &\Delta_{km} = 0, \text{for } k \neq i \text{ or } j \neq m. \end{aligned} \tag{69}$$

Therefore it is numerically shown that the system (68) is equivalent to (69). Although numerical calculations are not proof, they pave the way for finding the equal neigbouring eigenvalues (frequencies).

From this standpoint, it is unclear if there indeed is a repeated root or is this only a consequence of numerical error. This phenomenon is best seen on the graph showing the change of two neighbouring frequencies ω_n and ω_{n+1} with respect to the parameter D (Fig. 4). Without analytical proof, it is impossible to determine whether the curves are getting really close to each other and then veer away (*veering* phenomenon) or cross (*crossing* phenomenon). In the point where curves cross $\omega_n = \omega_{n+1}$ and a loss of a mode of vibration occurs. After the crossing, a swap of modes of vibration occurs due to the ordering convention.

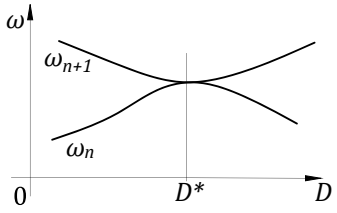

Figure 4: Illustration of *crossing* or *veering*.

The equality of two neighbouring frequencies implies the rank of the system matrix (50): $rank(\mathbf{K}(k^*, D^*)) = 1$. Let us assume that it is possible to determine the exact values of D^* and k^* from the following system of equations:

$$\begin{aligned} &\Delta_{11}(k^*, D^*) = 0, \\ &\Delta_{12}(k^*, D^*) = 0. \end{aligned} \tag{70}$$

To prove $rank(\mathbf{K}(k^*, D^*)) = 1$, it is sufficient to prove that all second order cofactors of matrix $\mathbf{K}$ are equal to zero. For this at our disposal we have the matrix elements (54)-(62) and also the relations between them (63)-(65).

When Δ_{11} and Δ_{12} are multiplied with $16D$, and Δ_{33} with $\frac{8}{k^*}$, we get the following equations:

$$\begin{aligned}
&Q_{11}(k^*, D^*) = 16D^*\Delta_{11} = 16D^*K_{22}K_{33} - K_{23}K_{32} = \\
&16a^2(Ch - Co)(Sh - Si) + b^2D^2k^{*2}(Ch + Co)(Sh - Si) - \\
&4abD^*k^*\left(\left(3 + 2\sqrt{2}\right)Ch^2 - \left(3 + 2\sqrt{2}\right)Co^2 + \left(3 + 2\sqrt{2}\right)Sh^2 - \left(6 - 4\sqrt{2}\right)ShSi + \left(3 + 2\sqrt{2}\right)Si^2\right) = 0, \\
&Q_{12}(k^*, D^*) = 16D^*\Delta_{12} = 16D^*K_{23}K_{31} - K_{21}K_{33} = \\
&16a^2(Ch - Co)^2 + b^2D^{*2}k^{*2}(Sh - Si)^2 - \\
&8abD^*k^*\left(Ch\left(3Sh + 2\sqrt{2}Sh - 3Si + 2\sqrt{2}Si\right) + Co\left(-3Sh + 2\sqrt{2}Sh + 3Si + 2\sqrt{2}Si\right)\right) = 0, \\
&Q_{33}(k^*, D^*) = \frac{8}{k^*}\Delta_{33} = 16D^*K_{11}K_{22} - K_{12}K_{21} = \\
&(3 + 2\sqrt{2})Ch^4 + (3 + 2\sqrt{2})Co^4 + (3 + 2\sqrt{2})Sh^4 + 4Sh^3Si + (18 - 4\sqrt{2})Sh^2Si^2 + 4ShSi^3 + (3 + 2\sqrt{2})Si^4 - \\
&2Ch^2\left(\left(3 + 2\sqrt{2}\right)Co^2 + \left(3 + 2\sqrt{2}\right)Sh^2 + 2ShSi + 3\left(1 - 2\sqrt{2}\right)Si^2\right) + \\
&Co^2\left(\left(6 - 12\sqrt{2}\right)Sh^2 + 4ShSi + 2\left(3 + 2\sqrt{2}\right)Si^2\right).
\end{aligned} \tag{71}$$

Substituting $Ch^2 = 1 + Sh^2$ and $Co^2 = 1 - Si^2$ into $Q_{33}(k^*, D^*)$, we get:

$$Q_{33}(k^*, D^*) = 16\sqrt{2}Si^2 + Sh^2\left(-16\sqrt{2} + 3\left(4 + 8\sqrt{2}\right)Si^2\right). \tag{72}$$

By analysing this system (70) of two quadratic equations in terms of a and b, it is possible to recognize the needed transformations to turn it into a homogenous system of linear equations:

$$\begin{aligned}
&(Q_{11}(Ch - Co) - Q_{12}(Sh - Si))\frac{1}{bD^*k^*} = 0, \\
&(Q_{11}(Sh - Si) - Q_{12}(Ch + Co))\frac{1}{4a} = 0,
\end{aligned} \tag{73}$$

which when simplified has the form:

$$\begin{aligned}
&B_{11}a - B_{12}b = 0, \\
&B_{21}a - B_{22}b = 0,
\end{aligned} \tag{74}$$

where:

$$\begin{aligned}
B_{11} = &-4\left(\left(3 + 2\sqrt{2}\right)Ch^3 - \left(3 + 2\sqrt{2}\right)Ch^2Co - \right. \\
&-Ch\left(\left(3 + 2\sqrt{2}\right)Co^2 + \left(3 + 2\sqrt{2}\right)Sh^2 - 2\left(3 + 2\sqrt{2}\right)ShSi + 3\left(1 - 2\sqrt{2}\right)Si^2\right) + \\
&\left.+Co\left(\left(3 + 2\sqrt{2}\right)Co^2 + \left(3 - 6\sqrt{2}\right)Sh^2 - 2\left(3 + 2\sqrt{2}\right)ShSi + \left(3 + 2\sqrt{2}\right)Si^2\right)\right), \\
B_{12} = &-Dk\left(-Ch^2 + Co^2 + (Sh - Si)^2\right)(Sh - Si), \\
B_{21} = &-4(Ch - Co)\left(Ch^2 - Co^2 - (Sh - Si)^2\right), \\
B_{22} = &+Dk\left(8\sqrt{2}ChCo(Sh + Si) + Ch^2\left(3Sh + 2\sqrt{2}Sh - 3Si + 6\sqrt{2}Si\right) + \right. \\
&+Co^2\left(\left(-3 + 6\sqrt{2}\right)Sh + \left(3 + 2\sqrt{2}\right)Si\right) - \\
&\left.-(Sh - Si)\left(\left(3 + 2\sqrt{2}\right)Sh^2 + 2\left(-3 + 2\sqrt{2}\right)ShSi + \left(3 + 2\sqrt{2}\right)Si^2\right)\right).
\end{aligned} \tag{75}$$

For (74) to have a non-trivial solution, the determinant of the system matrix **B** has to be equal to zero:

$$|\mathbf{B}| = \begin{vmatrix} B_{11} & -B_{12} \\ B_{21} & -B_{22} \end{vmatrix} = 0. \tag{76}$$

Using the known identities for triginometric and hyperbolic functions with *Co*, *So*, *Ch* and *Sh*:

$$Co^2 = 1 - Si^2, Ch^2 = 1 + Sh^2, Ch^3 = (1 + Sh^2)Ch, \tag{77}$$

we get:

$$|\mathbf{B}| = -4\sqrt{2}(Ch + Co)(Sh + Si)\left(16\sqrt{2}Si^2 + Sh^2\left(-16\sqrt{2} + 3\left(4 + 8\sqrt{2}\right)Si^2\right)\right) = 0. \tag{78}$$

Now the relation between $Q_{33}(k^*, D^*)$ and $|\mathbf{B}|$ is obvious:

$$|\mathbf{B}| = -4\sqrt{2}(Ch + Co)(Sh + Si)Q_{33}(k^*, D^*) = 0, \tag{79}$$

and knowing that the terms in brackets aren't equal to zero, the proof follows as:

$$Q_{33}(k^*, D^*) = 0 \Rightarrow \Delta_{33}(k^*, D^*) = 0 \Rightarrow K_{21} = \frac{K_{11}K_{22}}{K_{12}}. \tag{80}$$

4.1. Remaining cofactors

For k^* and D^*:

$$\Delta_{11}(k^*, D^*) = 0 \Rightarrow K_{22}K_{33} - K_{23}K_{32} = 0 \Rightarrow K_{22} = \frac{K_{23}K_{32}}{K_{33}}, \tag{81}$$

$$\Delta_{12}(k^*, D^*) = 0 \Rightarrow K_{23}K_{31} - K_{21}K_{33} = 0 \Rightarrow K_{21} = \frac{K_{23}K_{31}}{K_{33}}. \tag{82}$$

Substituting (81) and (82) into (67) for Δ_{13}:

$$\begin{aligned} \Delta_{13}(k^*, D^*) = K_{21}K_{32} - K_{22}K_{31} = \frac{K_{23}K_{31}}{K_{33}}K_{32} - \frac{K_{23}K_{32}}{K_{33}}K_{31} = 0 \Leftrightarrow \\ \Leftrightarrow K_{21}K_{32} - K_{22}K_{31} = 0. \end{aligned} \tag{83}$$

Substituting (63), (64) and (65) into (67) for Δ_{21}, while using (82):

$$\begin{aligned} \Delta_{21}(k^*, D^*) &= K_{13}K_{32} - K_{12}K_{33} = -\frac{D}{2}K_{31}kK_{23} + \frac{Dk}{2}K_{21}K_{33} \\ &= -\frac{Dk}{2}\left(K_{23}K_{31} - K_{21}K_{33}\right) = -\frac{Dk}{2}\Delta_{12} = 0 \Leftrightarrow \\ &\Leftrightarrow K_{13}K_{32} - K_{12}K_{33} = 0 \Rightarrow K_{12} = \frac{K_{13}K_{32}}{K_{33}}. \end{aligned} \tag{84}$$

Substituting (84) and (81) into (67) for Δ_{31}:

$$\begin{aligned} \Delta_{31}(k^*, D^*) =& K_{12}K_{23} - K_{13}K_{22} = \frac{K_{13}K_{32}}{K_{33}}K_{23} - K_{13}\frac{K_{23}K_{32}}{K_{33}} = 0 \Leftrightarrow \\ \Leftrightarrow& K_{12}K_{23} - K_{13}K_{22} = 0. \end{aligned} \tag{85}$$

Substituting (85) and (80) into (67) for Δ_{32}:

$$\begin{aligned} \Delta_{32}(k^*, D^*) =& K_{13}K_{21} - K_{11}K_{23} = K_{13}\frac{K_{11}K_{22}}{K_{12}} - K_{11}\frac{K_{13}K_{22}}{K_{12}} = 0 \Leftrightarrow \\ \Leftrightarrow& K_{13}K_{21} - K_{11}K_{23} = 0. \end{aligned} \tag{86}$$

From (80), using (85) and (82) it follows that:

$$\begin{aligned}\Delta_{33}(k^*, D^*) &= K_{11}K_{22} - K_{12}K_{21} = K_{11}\frac{K_{12}K_{23}}{K_{13}} - K_{12}K_{21} = K_{11}\frac{K_{12}}{K_{13}}\frac{K_{21}K_{33}}{K_{31}} - K_{12}K_{21} \\ &= \frac{K_{12}K_{21}}{K_{13}K_{31}}(K_{11}K_{33} - K_{13}K_{31}) = \frac{K_{12}K_{21}}{K_{13}K_{31}}\Delta_{22}(k^*, D^*) \Rightarrow \Delta_{22}(k^*, D^*) = 0.\end{aligned} \tag{87}$$

Substituting (84) and (87) into (67) for Δ_{23}:

$$\begin{aligned}\Delta_{23}(k^*, D^*) =& K_{12}K_{31} - K_{11}K_{32} = \frac{K_{13}K_{32}}{K_{33}}K_{31} - \frac{K_{13}K_{31}}{K_{33}}K_{32} = 0 \Leftrightarrow \\ \Leftrightarrow& K_{12}K_{23} - K_{13}K_{22} = 0.\end{aligned} \tag{88}$$

This is the proof that $rank(\mathbf{K}) = 1$ for the diameter D^* and characteristic number k^* which can be determined numerically from (70).

4.2. Numerical example

A numerical calculation was done in *Wolfram Mathematica* to show the crossing phenomenon. From sections (4) and (4.1), namely eqs. (80), (84) and (87) for example, we see that there are six independent cofactors of the **K** matrix. For the problem formulated in Chapter 2, a length of 1 meter is assigned to both beam elements, and numerical solutions k and D are found for $\Delta_{ij}(\,k, D) \;= 0$ for six independent cofactors: $\Delta_{11}, \Delta_{12}, \Delta_{13}, \Delta_{21}, \Delta_{23}$ and Δ_{33}. A contour plot is given in Fig. (5(a)) for proposed ranges of k and D, where within a numerical error, a $k^* = 7.06111\frac{1}{\mathrm{m}}$ and $D^* = 0.05690$ m are found to satisfy all of the six equations simultaneously. This result presents the third and fourth frequencies k_3 and k_4 being equal. The Euler-Bernoulli theory is applicable within the diameter range $D \leq 0.1$ m for a beam of 1 meter in length. In Fig. 5(b) a contour plot of $|\mathbf{K}(k, D)| = 0$ is given, with curves labeled k_i for $i = 1, 2, 3, \ldots$, which show the change of characteristic numbers with varying the diameter D.

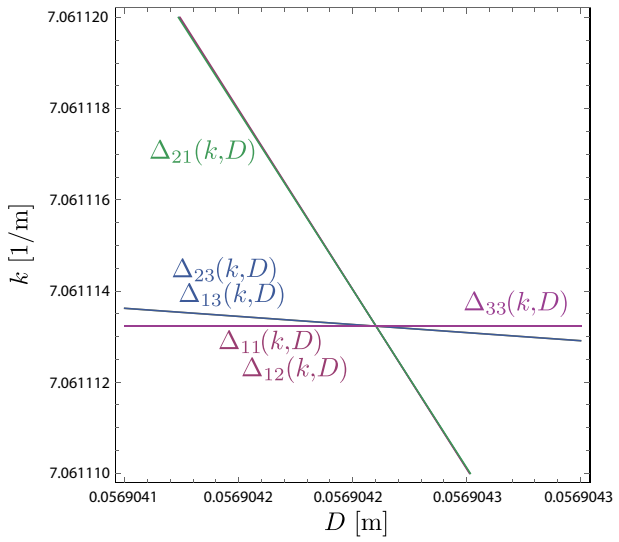

(a) Contour plots of $\Delta_{ij}(\,k, D) \;= 0$.

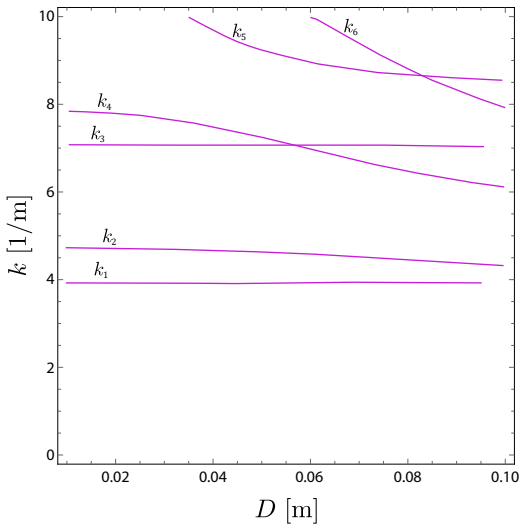

(b) Contour plot of $|\mathbf{K}(k, D)| = 0$.

5. Conclusion

This paper concerned crossing and veering eigenvalue phenomena in frames by following analytical procedures. The general analytical model based on the Euler-Bernoulli beam theory is implemented and

eigenvalue changes are observed by varying the diameter of comprising beams. The existence of axial and transverse mode shapes coupling is presented. When solving the governing equations for each beam authors observed a connection between coefficients that reduces to the third order system of linear equations with respect to coefficients. The system matrix is analyzed following the laws of linear algebra. Based on the rank of the system matrix, it is shown that eigenvalue loci intersect and crossing occurs since the rank of the system matrix is derived to be 1 for the predetermined values of k and D. In that manner the purpose of this paper is obtained to show analytically that eigenvalue crossing occurs. The paper only gives insight that it is possible to determine an analytical requirement for the appearance of crossing from a simple mathematical condition for a specific and symmetric model. Many more complex examples of discrete and continuous models exist which can be examined more thoroughly to find patterns of occurence of crossing and veering and define righorous mathematical conditions for their existence.

References

[1] A. Tomović, S. Šalinić, A. Obradović, A. Grbović, M. Milovančević, *Closed-form solution for the free axial-bending vibration problem of structures composed of rigid bodies and elastic beam segments*, J. Appl. Math. Model. **77** (2020), 1148-1167, https://doi.org/10.1016/j.apm.2019.09.008.

[2] J.L. du Bois, S. Adhikari, N.A.J. Lieven, *On the Quantification of Eigenvalue Curve Veering: A Veering Index*, J. Appl. Mech. **78(4)**, (2011), pp. 041007.

[3] B.R. Mace, E. Manconi, *Mode veering in weakly coupled systems*, Int. Conf. Noise Vib. Eng. 2012, ISMA 2012, Incl. USD 2012 Int. Conf. Uncertain. Struct. Dyn. 4, 3211-3222 (2012)

[4] A. Obradović, S. Šalinić, A. Tomović, *Free Vibrations of Planar Serial Frame Structures in the Case of Axially Functionally Graded Materials*, J. Appl. Mech. **47** (2020), 221-239, https://doi.org/10.2298/TAM2000017O.

[5] J. Fang, D. Zhou, *In-plane vibration analysis of rotating tapered timoshenko beams*, Int. J. Appl. Mech. **8** (2016), 221-239, https://doi.org/10.1142/S1758825116500642.

[6] Y. Zhang, Y. Petrov, Y.P. Zhao, *Eigenfrequency loci crossings, veerings and mode splittings of two cantilevers coupled by an overhang*, J. Phys. Commun. **4** (2020), 1-16, https://doi.org/10.1088/2399-6528/abab3f.

[7] C. Pierre, *Mode Phenomena and Eigenvalue Loci Veering*, J. Sound Vib. **126** (1988), 485-502.

[8] E. Manconi, B. Mace, *Veering and Strong Coupling Effects in Structural Dynamics*, J. Vib. Acoust. Trans. ASME. **139(2)**, 021009-10, (2017), https://doi.org/10.1115/1.4035109.

[9] X. Chen, A. Kareem, *Curve Veering of Eigenvalue Loci of Bridges with Aeroelastic Effects*, J. Eng. Mech. **129** (2003), 146-159, https://doi.org/10.1061/(asce)0733-9399(2003)129:2(146).

[10] E. Bonisoli, C. Delprete, M. Esposito, J.E. Mottershead, *Structural dynamics with coincident eigenvalues: Modelling and testing*, Conf. Proc. Soc. Exp. Mech. Ser. **3** (2011), 325-337, https://doi.org/10.1007/978-1-4419-9299-4_29

[11] J.L. du Bois, S. Adhikari, N.A.J. Lieven, *Eigenvalue curve veering in stressed structures: An experimental study*, J. Sound Vib. **322(4-5)**, (2009), 1117–1124.

[12] S. Tornincasa, E. Bonisoli, P. Kerfriden, M. Brino, *Investigation of crossing and veering phenomena in an isogeometric analysis framework*, Conf. Proc. Soc. Exp. Mech. Ser. **8** (2014), 361-376, https://doi.org/10.1007/978-3-319-04774-4_34

[13] A. Galina, L. Pichler, T. Uhl, *Enhanced meta-modelling technique for analysis of mode crossing, mode veering and mode coalescence in structural dynamics*, Mech. Syst. Signal Process. **25** (2011), 2297-2312, https://doi.org/10.1016/j.ymssp.2011.02.020.

[14] B.B. Bhat, *Curve veering: Inherent behaviour of some vibrating systems*, J. Shock Vib. **7** (2000), 241-249, https://doi.org/10.1155/2000/841538.

[15] O. Giannini, A. Sestieri, *Experimental characterization of veering crossing and lock-in in simple mechanical systems*, Mech. Syst. Signal Process. **72-73** (2016), 846-864, https://doi.org/10.1016/j.ymssp.2015.11.012.

[16] E. Bonisoli, M. Brino, C. Delprete, *Numerical-experimental comparison of a parametric test-rig for crossing and veering phenomena*, Mech. Syst. Signal Process. **128** (2019), 369-388, https://doi.org/10.1016/j.ymssp.2019.03.039.

[17] Y. Zhang, Y. Petrov, Y.P. Zhao, *Mode localization and eigenfrequency curve veerings of two overhanged beams*, Micromachines **12** (2021), 1-19, https://doi.org/10.3390/mi12030324.

[18] C. Pierre, *Mode localization and eigenvalue loci veering phenomena in disordered structures*, J. Sound Vib. **126** (1988), 485-502, https://doi.org/10.1016/0022-460X(88)90226-X.

[19] X.L. Liu, *Behavior of derivatives of eigenvalues and eigenvectors in curve veering and mode localization and their relation to close eigenvalues*, J. Sound Vib. **256** (2002), 551-564,https://doi.org/10.1006/jsvi.2002.5010.

[20] V. Ondra, B. Titurus, *Free vibration and stability analysis of a cantilever beam axially loaded by an intermittently attached tendon*, Mech. Syst. Signal Process. **158**, (2021), 551-564, https://doi.org/10.1016/j.ymssp.2021.107739.

[21] N.G. Stephen, *On veering of eigenvalue loci*, J. Vib. Acoust. Trans. ASME. **131**, 0545011–0545015, (2009), 551-564, https://doi.org/10.1115/1.3147130.

[22] D. Karličić, M. Cajić, T. Chatterjee, S. Adhikari, *Wave propagation in mass embedded and pre-stressed hexagonal lattices*, J. Compos. Struct. **256**, (2021), https://doi.org/10.1016/j.compstruct.2020.113087.

[23] SS. Rao, *Vibration of continuous systems*, New Jersey: Wiley; 2007.